Paeoniflorigenone inhibits ovarian cancer metastasis through targeting the MUC1/Wnt/β-catenin pathway

QINGLING LIU[1*], LIQIN JIANG[1*], YUN ZHAO[1], FANG SU[1], JUNFENG LI[1], XINXIN TIAN[2], WENHONG LIU[1], XIAWEI JIANG[1], YE XU[1] and FANGFANG TAO[1]

[1]Department of Immunology and Microbiology, School of Basic Medical Sciences, Zhejiang Chinese Medical University, Hangzhou, Zhejiang 310053, P.R. China; [2]Department of Human Cell Biology and Genetics, School of Medicine, Southern University of Science and Technology, Shenzhen, Guangdong 518055, P.R. China

Received April 25, 2023; Accepted December 13, 2023

DOI: 10.3892/ijmm.2024.5384

Abstract. Ovarian cancer (OC) is one of the most common gynecological malignancies. Currently, chemoradiotherapy is the primary clinical treatment approach for OC; however, it has severe side effects and a high rate of recurrence. Thus, there is an urgent need to develop innovative therapeutic options. Paeoniflorigenone (PFG) is a monoterpene compound isolated from the traditional Chinese medicine Paeoniae Radix Rubra. PFG can inhibit the proliferation of tumor cells; however, its anticancer activity against OC has yet to be elucidated. Mucin 1 (MUC1) is highly expressed in various malignant tumors, and is associated with tumor proliferation, metastasis and epithelial-mesenchymal transition (EMT). In addition, MUC1 affects numerous signaling pathways in tumor cells. In order to develop a possible treatment approach for metastatic OC, the antitumor activity of PFG in OC cells was investigated using Cell Counting Kit-8 assay, Edu assay, flow cytometry, Transwell assay and western blot analysis. In addition, it was assessed how PFG affects MUC1 expression and function. The experiments revealed that PFG significantly inhibited OC cell proliferation, migration, invasion and EMT. PFG also induced S-phase cell cycle arrest in OC cells. Furthermore, PFG inhibited MUC1 promoter activity, which led to a decrease in MUC1 protein expression. By contrast, MUC1 promoted OC progression, including cell proliferation, cell cycle progression and cell migration. Stable knockdown of MUC1 in OC cells improved the ability of PFG to block the Wnt/β-catenin pathway, and to limit tumor cell invasion and migration, whereas MUC1 overexpression partially counteracted the antitumor effects of PFG. In conclusion, the present study demonstrated that PFG may inhibit the MUC1/Wnt/β-catenin pathway to induce anti-metastatic, anti-invasive and anti-EMT effects on OC. Notably, MUC1 may be a direct target of PFG. Thus, PFG holds promise as a specific antitumor agent for the treatment of OC.

Correspondence to: Professor Fangfang Tao or Dr Ye Xu, Department of Immunology and Microbiology, School of Basic Medical Sciences, Zhejiang Chinese Medical University, 548 Puyan Street, Hangzhou, Zhejiang 310053, P.R. China
E-mail: taoff@zcmu.edu.cn
E-mail: crafy@qq.com

*Contributed equally

Abbreviations: OC, ovarian cancer; PFG, paeoniflorigenone; MUC1, mucin 1; EMT, epithelial-mesenchymal transition; TCM, traditional Chinese medicine; PRR, Paeoniae Radix Rubra; FBS, fetal bovine serum; CCK-8, Cell Counting Kit-8

Key words: paeoniflorigenone, ovarian cancer, mucin 1, metastasis, Wnt/β-catenin pathway

Introduction

Ovarian cancer (OC) is a major health concern among women worldwide, ranking as the seventh most commonly diagnosed cancer and the eighth leading cause of cancer-associated death (1,2). By the end of 2023, it is predicted that 19,710 new OC cases will be diagnosed and 13,270 OC-related deaths will occur in the United States (3). OC is considered the most lethal gynecological cancer due to its asymptomatic early stages and the inadequate screening methods for detecting precancerous lesions, often resulting in a late-stage diagnoses (at stage III/IV). In addition to traditional surgery, the treatment options for OC include platinum-based combined chemotherapy and radiotherapy (4). Most patients are treated with surgery first, followed by platinum-based combined chemotherapy (5). However, it has been reported that both chemotherapy and radiotherapy have serious side effects (6), and tumor recurrence arises as a result of treatment resistance (7). Therefore, identifying novel therapeutic strategies is crucial to treat OC.

Traditional Chinese medicine (TCM) has a history of 2,500 years and has been used to treat diseases since ancient times (8). Paeoniae Radix Rubra (PRR, also known as Chishao) is a type of Chinese herbal medicine, which is the dried root of *Paeonia lactiflora* Pall. PRR is often used in TCM formulations to clinically treat cancer (9,10), such as the Guizhi Fuling Formulation (11) for the treatment of bladder cancer, OC and breast cancer. Paeoniflorin has been identified as one of the main components in PRR with antitumor activity (12).

A water-soluble monoterpene glycoside known as paeoniflorin has been reported to have a good antitumor function in various types of cancer, such as liver cancer (13), gastric cancer (14), breast cancer (15), lung cancer (16) and bladder cancer (12), and the molecular mechanisms involved include the nuclear factor κB, STAT3 and p53/14-3-3 signaling pathways (17).

Paeoniflorigenone (PFG), another monoterpene compound found in *Paeonia* species, has been shown to possess a range of bioactive properties. Previous research has shown that PFG is a depolarizing neuromuscular blocking agent in frogs and mice, being similar to succinylcholine (18). PFG can also improve blood circulation through anticoagulant and anti-platelet activities (19). In addition, it has been reported that PFG induces Jurkat cells, HeLa cells and HL-60 tumor cell lines to undergo apoptosis, possibly through the activation of caspase-3 (20). Additionally, PFG can suppress the growth of cancerous HeLa cells through triggering S and G_2/M cell cycle arrest and inhibiting mitosis (21). Nevertheless, to the best of our knowledge, the mechanism underlying the antitumor activity of PFG in OC has not been reported.

Over 90% of cases of epithelial OC (EOC), including platinum-resistant tumors, exhibit upregulation of the type I transmembrane glycoprotein mucin 1 (MUC1), which is highly glycosylated (22,23). Following O-glycosylation and N-glycosylation, MUC1 matures into a mucin that is capable of performing its function (24). Glycosylation is thought to be responsible for 50-90% of the total weight of MUC1, and MUC1 can range in weight from 250 to 500 kDa, depending on the quantity of tandem repeats and the level of glycosylation (25). Notably, MUC1 can serve as a target and prognostic biomarker for immunotherapy (26). Overexpression of MUC1 has been shown to promote the invasive growth and metastasis of tumor cells (27,28). Furthermore, MUC1 functions as an anti-adhesion factor in cancer, and may destroy cell-to-cell and cell-to-matrix adhesion, releasing cells from tumor nests and causing micro-metastasis (29,30). Additionally, MUC1 induces epithelial-mesenchymal transition (EMT) at the post-transcriptional level by altering the expression of microRNAs that regulate the expression of EMT-related genes (31,32). As a result, tumor-associated MUC1 represents a prospective therapeutic target for EOC.

The present study aimed to scrutinize the inhibitory effect of PFG on SKOV3 and A2780 OC cells, and to investigate the role of MUC1 in the anti-OC effects of PFG by knocking down and overexpressing MUC1.The present study also explored the association of MUC1 expression with the pharmaceutical effectiveness of PFG, potentially providing a new approach for developing MUC1-targeted drugs.

Materials and methods

Cell culture. China Center for Type Culture Collection supplied the human OC cell lines SKOV3, A2780 and HEY-T30. SKOV3 cells were grown in McCoy's 5A medium (Cienry Biotechnology, Inc.), whereas A2780 and HEY-T30 cells were grown in RPMI 1640 medium (Gibco; Thermo Fisher Scientific, Inc.). Both media were supplemented with 10% (v/v) fetal bovine serum (FBS; Invigentech, Inc.), 100 U/ml penicillin and 100 μg/ml streptomycin (Beyotime Institute of Biotechnology). The cells were grown at 37˚C in an atmosphere containing 5% CO_2 with saturated humidity.

Reagents and antibodies. PFG (cat. no. B31203; molecular weight: 318.326; purity ≥98%; lot no. D15GB171320; Fig. 1A) was purchased from Shanghai Yuanye Bio-Technology Co., Ltd. PFG was mixed with dimethyl sulfoxide and stored at -80˚C. To reduce the effects of serum and other chemicals in the culture medium on pharmacological action, PFG was diluted in cell culture medium containing 2% FBS and applied in all experiments. Docetaxel (cat. no. HY-B0011; purity 99.42%) was purchased from MedChemExpress, and was used to treat SKOV3 and A2780 cells for 24 h at 37˚C at a dose of 80 nM. The Wnt/β-catenin pathway inhibitor XAV939 (cat. no. S1180; molecular weight: 312.31; purity 99.95%) was purchased from Selleck Chemicals, which was used to treat SKOV3 and A2780 cells for 24 h at 37˚C at a dose of 10 μM. The MUC1 (cat. no. 4538S), N-cadherin (cat. no. 13116S), Vimentin (cat. no. 5741S), Snail (cat. no. 3879S), β-catenin (cat. no. 8480S) and cyclin D1 (cat. no. 55506S) antibodies were purchased from Cell Signaling Technology, Inc. Antibodies against MMP2 (cat. no. ab92536), MMP9 (cat. no. ab76003) and CDK2 (cat. no. ab32147) were acquired from Abcam. Antibodies against c-Myc (cat. no. sc-40), cyclin A (cat. no. sc-239) and cyclin E (cat. no. sc-247) were obtained from Santa Cruz Biotechnology, Inc. The β-actin antibody (cat. no. AC026) was obtained from ABclonal, Inc. HRP-conjugated goat anti-mouse IgG H&L (cat. no. BK-M050) and anti-rabbit IgG H&L (cat. no. BK-R050) antibodies were purchased from BIOKER Biotechnology, Inc. For western blotting, antibodies were used at a 1:1,000 dilution.

Molecular docking. The Research Collaboratory for Structural Bioinformatics Protein Data Bank database (https://www.rcsb.org/) and the PubChem database (https://pubchem.ncbi.nlm.nih.gov/) were utilized to find the three-dimensional structures of the MUC1 protein and molecular ligand structures, respectively. The Dockthor tool (https://docthor.lncc.br/v2/) was used to process proteins and ligands, including removing water molecules, performing hydrogenation and calculating protein charges. The final docking conformation should have the strongest affinity. According to this principle, the conformation was selected and visualized using Pymol 2.3 software (33).

Cell counting kit-8 (CCK-8) assay. Cell proliferation and the drug half maximal inhibitory concentration (IC_{50}) were examined by CCK-8 assay (Biosharp Life Sciences). SKOV3 and A2780 cells were inoculated in 96-well plates at a density of $4x10^3$ cells/well. The cells were incubated overnight with 5%CO_2 at 37˚C in 5% CO_2, and were then treated with various doses of PFG (0, 0.5, 1, 2, 5, 10, 20 and 40 μM) for 24, 48 and 72 h at 37˚C. As recommended, 10 μl CCK-8 reagent was then added per well and incubated for 1 h at 37˚C in 5% CO_2. A New Epoch™ 2 Epoch Microplate Spectrophotometer (Thermo Fisher Scientific, Inc.) was used to measure the absorbance at 450 nm.

Colony formation assay. SKOV3 and A2780 cells were exposed to different concentrations of PFG (0.5, 1 and 2 μM)

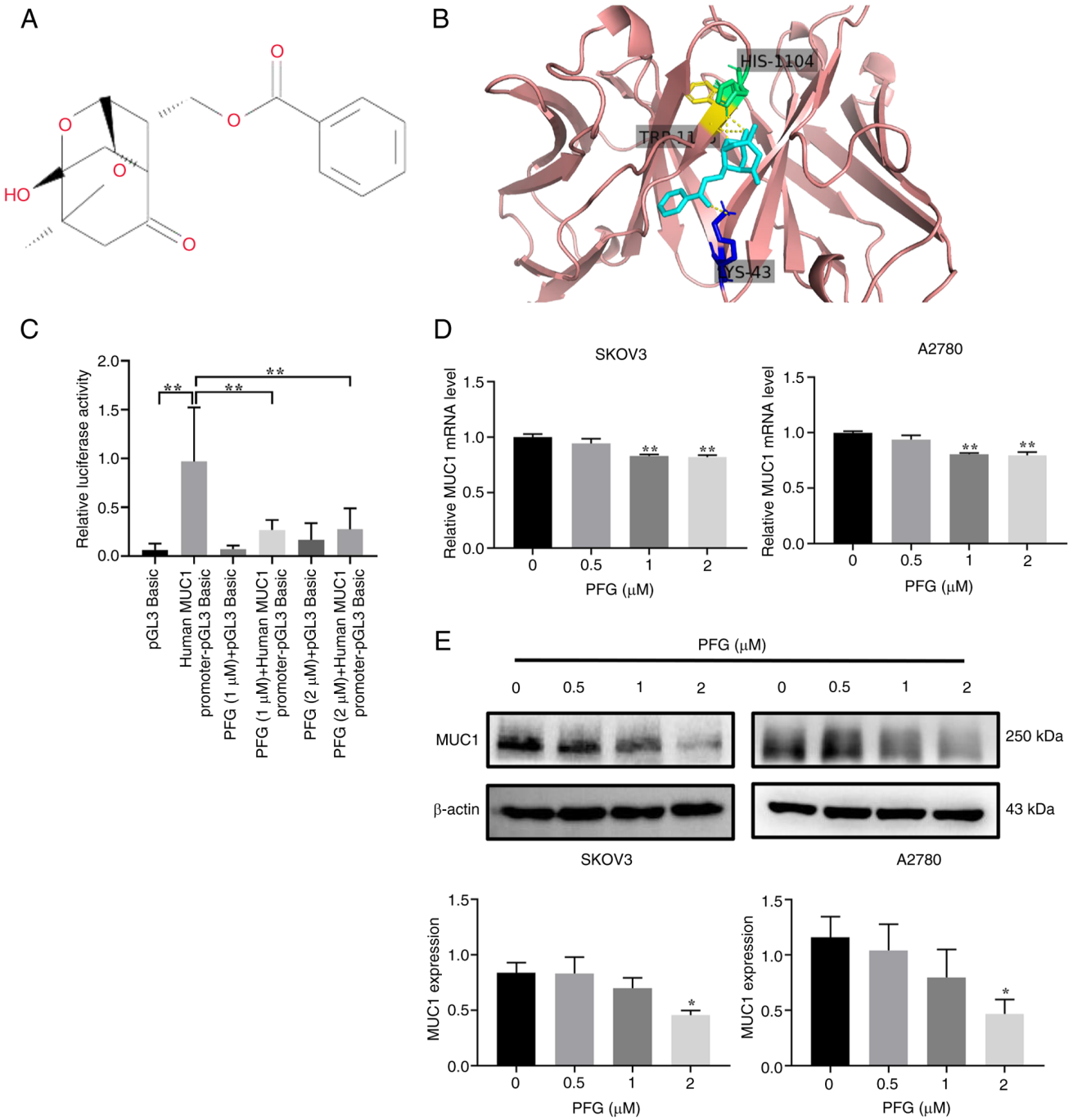

Figure 1. PFG inhibits the expression of MUC1 in ovarian cancer cells. (A) Chemical structure of PFG. (B) Binding mode of PFG with MUC1. Pink depicts the three-dimensional structure of MUC1; blue indicates the PFG structure; yellow, green, and dark blue correspond to distinct amino acid residues and the amino acid residue appears in black type. (C) PFG inactivates the MUC1 promoter in SKOV3 cells. (D) Reverse transcription-quantitative polymerase chain reaction detection of MUC1 mRNA expression levels in response to different PFG doses. GAPDH was used as an internal control. (E) Changes in MUC1 protein expression levels in response to PFG treatment in SKOV3 and A2780 cells, as determined by western blotting. β-actin was used as an internal control. Data are presented as the mean ± SEM (n=3) and one-way ANOVA was used to determine statistical significance. *P<0.05, **P<0.01 vs. control group or as indicated. MUC1, mucin 1; PFG, paeoniflorigenone.

for 24 h at 37˚C in 5% CO_2, then grown in McCoy's 5A or RPMI 1640 media supplemented with 10% FBS for 2 weeks, after being plated at a density of 1,000 cells/well in 6-well plates. Subsequently, 4% paraformaldehyde was employed to fix the colonies for 20 min and they were stained with 0.1% crystal violet for 30 min at room temperature. An optical microscope was used to count colonies containing >50 cells.

EdU assay. Using an EdU assay kit (Beyotime Institute of Biotechnology), the cell proliferation capacity was detected. At a density of $4x10^5$ cells/well, cells were plated into 6-well plates and exposed to different concentrations of PFG (0.5, 1 and 2 μM) for 24 h at 37˚C in 5% CO_2. After SKOV3 and A2780 cells underwent a 2 h incubation in 50 μM EdU buffer at 37˚C in 5% CO_2, they were fixed for 30 min in 4% paraformaldehyde, and then permeabilized for 20 min in 0.1% Triton

X-100. After the culture was infused with click reaction solution, prepared according to the manufacturer's instructions, and then incubated in the dark for 30 min at room temperature, the nuclei were stained with 1X Hoechst 33342 at room temperature in the dark for 10 min. A fluorescence microscope was used to visualize the cells.

Cell cycle and apoptosis assay. To analyze cell apoptosis, the Annexin-V FITC/PI Apoptosis Analysis Kit (Beyotime Institute of Biotechnology) was used. Several concentrations of PFG (0.5, 1 and 2 μM) were used to pretreat SKOV3 and A2780 cells for 24 h at 37˚C in 5% CO_2. According to the manufacturer's instructions, prior to staining with 5 μl Annexin-V/FITC and 10 μl PI at room temperature in the dark for 15 min, centrifuged cells (1,000 x g for 5 min at 25˚C) were rinsed in precooled PBS. In addition, as a positive control, cells were treated with 80 nM docetaxel for 24 h at 37˚C in 5% CO_2. To assess cell cycle progression, the Cell Cycle Analysis Kit (Shanghai Yuanye Bio-Technology Co., Ltd.) was performed. The same cells were assessed as for the apoptosis experiment. According to the manufacturer's instructions, centrifuged cells (1,000 x g for 5 min at 25˚C) were rinsed gently in precooled PBS before being stained with 500 μl 50 μg/ml PI staining reagent (containing 200 μg/ml RNase) at room temperature in the dark for 15 min. The test was repeated three times for each sample. Finally, FlowJo-V10 software (FlowJo, LLC) was used to investigate the apoptosis and cell cycle data, which were collected using Beckman CytoFlex (Beckman Coulter, Inc.). The apoptotic rate was calculated using the formula: Apoptotic rate=Q1-LR + Q1-UR. LR refers to early apoptotic rate and UR to late apoptotic rate.

DNA fragmentation analysis. DNA fragmentation, which is a hallmark of apoptosis, was studied using the One-Step TUNEL Apoptosis Detection Kit (FITC) (MedChemExpress). SKOV3 and A2780 cells ($2x10^4$/well) were seeded in 24-well plates and treated with PFG (0.5, 1 and 2 μM) or docetaxel (80 nM) at 37˚C in 5% CO_2 for 24 h. Cells were fixed with 10% neutral buffered formalin at room temperature for 20 min, and stained according to the manufacturer's protocol. Slides were then cover-slipped with antifade mounting medium with DAPI (Vector Laboratories, Inc.). Images were acquired using a fluorescence microscope, and the fluorescence intensity was statistically analyzed by ImageJ v1.48 software (National Institutes of Health). The experiment was repeated three times.

Wound-healing assay. OC cells ($3x10^6$ cells/well) were plated on 6-well plates and allowed to adhere to the plates for 24 h. To maintain a healthy cell growth state, when the fusion degree of the cell monolayer reached >80%, a straight line was scratched into the monolayer using a 200-μl pipette tip. After three washes with PBS, PFG (0.5, 1 and 2 μM) with 2% FBS was added to each plate at 37˚C in 5% CO_2 for 24 h. The distance that cells had migrated was photographed under a light microscope at 0, 12 and 24 h for the subsequent calculation. Taking 24 h as an example, migration was assessed as follows: Migration rate (%)=(At=0 h)-(At=24 h)/(At=0 h). (At=0 h) refers to the area of the wound measured immediately after scratching; (At=24 h) refers to the area of the wound measured 24 h after the scratch was performed.

Migration and invasion assays. For the migration and invasion assays, PFG was applied to SKOV3 and A2780 at 0.5, 1 and 2 μM at 37˚C in 5% CO_2 for 24 h. Subsequently, the upper chamber of a Transwell system (pore size, 8 μm; Corning, Inc.) was seeded with $2x10^4$ cells resuspended in 100 μl serum-free medium, and the bottom of the chamber contained the cell culture medium with 10% FBS. After the cells had migrated for 24 h at 37˚C in 5% CO_2, the chamber was removed, the unmigrated cells were scraped off, and the migrated cells were fixed with 4% paraformaldehyde for 20 min at room temperature and stained with 0.01% crystal violet (Beijing Solarbio Science & Technology Co., Ltd.) for 15 min at room temperature. Using a light microscope (x200 magnification; Olympus Corporation) cell images were captured and cell counts from five random fields were measured. For the invasion assay, the upper chamber of the insert was coated with 100 μl growth factor-reduced Matrigel (Corning, Inc.) overnight at 37˚C.

Establishment of stable cell lines with MUC1 knockdown and overexpression. To infect the SKOV3 and A2780 cell lines, Shanghai GeneChem Co., Ltd. provided both the lentivirus-based short hairpin (sh) RNA vector GV493 (hU6-MCS-CBh-gcGFP-IRES-puromycin) and the lentivirus-based overexpression RNA vector GV721 (CMV enhancer-MCS-3FLAG-EF1a-firefly_Luciferase-SV40-puromycin). According to the manufacturer's instructions, the recombined GV493/GV721 lentiviral vector plasmid or the negative control lentiviral vector plasmid, and pHelper 1.0 and pHelper 2.0 plasmids (Shanghai Genechem Co., Ltd.) were co-transfected into 293T cells (American Type Culture Collection) using HitransG enhanced infection solution (Shanghai Genechem Co., Ltd.) at 37˚C in 5% CO_2 for 6 h. Subsequently, the culture supernatant was removed and replaced with fresh high-glucose DMEM supplemented with 10% FBS and the culture supernatants were collected at 48 h post-transfection. Following centrifugation at 4,000 x g for 10 min at 4˚C to remove cell debris, the supernatant was filtered through 0.45-μm filters. The concentrated viral supernatant was aliquoted and maintained at -80˚C prior to use. The lentivirus was then diluted with serum-free McCoy's 5A or 1640 medium and used to infect SKOV3 and A2780 cells at a multiplicity of infection of 10. After 8 h at 37˚C in 5% CO_2, the medium was refreshed. Subsequently, at 72 h post-infection, puromycin (2 μg/ml) was employed to screen out the stable knockdown and overexpression cell lines at 37˚C in 5% CO_2 for 48 h, and then 1 μg/ml puromycin was used for maintenance. Finally, the SKOV3 and A2780 cells were harvested for further analysis. The following shRNA sequences were used: sh-MUC1, 5'-CCGGGATACCTACCATCCTATP-3'; sh-Control (non-targeting negative control viral vector), 5'-TTCTCCGAACGTGTCACGT-3'.

Promoter-reporter assays. According to the manufacturer's protocol, the pGL3 Basic human MUC1 promoter (HIBio Biotechnology Co., Ltd.) was transfected into human OC SKOV3 cells using Lipofectamine® 3000 Transfection Reagent (Invitrogen; Thermo Fisher Scientific, Inc.). As an internal control, a pRL-TK plasmid carrying the *Renilla* luciferase gene (HIBio Biotechnology Co., Ltd.) was co-transfected with pGL3 Basic human MUC1 promoter in SKOV3 cells.

Briefly, 24-well plates were used for transfection; the plasmid was transfected into cells at 37˚C in 5% CO_2 for 8 h, then the medium was replaced with fresh culture medium for 24 h. Subsequently, PFG (1 and 2 μM) was added for 24 h at 37˚C in 5% CO_2. Utilizing the Dual-luciferase Reporter Assay Kit (Promega Corporation), according to the guidelines provided by the manufacturer, cells transfected with vector were added to perform luciferase assays in triplicate in 96-well plates after puromycin resistance screening. GraphPad Prism 8 (Dotmatics) was used to evaluate and plot the exported data.

Reverse transcription-quantitative polymerase chain reaction (RT-qPCR) analysis. Using TRIzol® reagent (Invitrogen; Thermo Fisher Scientific, Inc.), RNA was extracted from the cells. The Nanodrop 2000 system (Thermo Fisher Scientific, Inc.) was employed to measure the quality and quantity of RNA. Subsequently, 1 μg total RNA was used to generate cDNA using the PrimeScript RT reagent kit (Takara Bio, Inc.) according to the manufacturer's protocol. qPCR was conducted on a CFX96 Real-Time PCR Detection System (Bio-Rad Laboratories, Inc.) using the SYBR Premix Ex Taq™ kit (Takara Bio, Inc.). The thermocycling conditions were as follows: An initial denaturation step at 95˚C for 10 sec, followed by 40 cycles, (denaturation at 95˚C for 10 sec, annealing at 64˚C for 25 sec), and a final extension step at 55˚C for 1 min and 95˚C for 10 sec. GAPDH was used as an internal control. To obtain the relative gene expression levels, the $2^{-\Delta\Delta Cq}$ method (34) was used. The following primer sequences were used: MUC1, forward 5'-ATACCTACCATCCTATGAG CGA-3', reverse 5'-CTGCTGGGTTTGTGTAAGAGA-3'; and GAPDH, forward 5'-GGTGGTCTCCTCTGACTTCAACA-3' and reverse 5'-GTTGCTGTAGCCAAATTCGTTGT-3'.

Western blotting. Cells were lysed in RIPA buffer with a proteinase inhibitor cocktail (Beyotime Institute of Biotechnology), and the BCA Protein Assay Kit (Thermo Fisher Scientific, Inc.) was used to quantify the amount of protein in the extracts. Proteins (20 μg) were separated by SDS-PAGE on 8% gels and were then transferred to polyvinylidene fluoride membranes (MilliporeSigma). To prevent nonspecific binding, the membranes were blocked for 2 h with 5% skim milk (Bio-Rad Laboratories, Inc.) diluted in Tris-buffered saline. Prior to being incubated with HRP-conjugated secondary antibodies at room temperature for 2 h, membranes were pre-incubated with a specific primary antibody for an overnight period at 4˚C. An ECL Western Blotting Detection kit (Biosharp Life Sciences) was utilized for detecting protein signals. After standardization to β-actin, ImageJ v1.48 software (National Institutes of Health) was used to measure the optical density of the blot.

Statistical analysis. GraphPad Prism version 8 software was used to investigate statistical significance via a Student's unpaired t-test, one-way ANOVA or two-way ANOVA with a Bonferroni multiple comparisons test (if the variance is homogeneous) or Games-Howell multiple comparison test (if the variance is uneven). All studies were conducted at least in triplicate, and all data are presented as the mean ± SEM. $P<0.05$ was considered to indicate a statistically significant difference.

Results

PFG inhibits the expression of MUC1 in OC cells. The binding mode of PFG to MUC1 was predicted by molecular docking, and it was revealed that PFG formed three hydrogen bonds with HIS-1104, LYS-43 and TRP-1105 amino acid residues (Fig. 1B). These results indicated that MUC1 is a potential target protein of PFG. Next, the effects of PFG on the promoter activity of MUC1 were assessed using a dual-luciferase assay. Compared with the human MUC1 promoter-pGL3 Basic group, the PFG (1 and 2 μM) groups showed a significant decrease in relative fluorescence activity, indicating that PFG treatment affected the binding of transcription factors to the MUC1 promoter in SKOV3 cells (Fig. 1C). Subsequently, quantification of MUC1 expression in SKOV3 and A2780 cells was performed using RT-qPCR and western blotting. The results suggested that PFG inhibited MUC1 expression and exhibited a concentration-dependent effect on the downregulation of MUC1 expression at concentrations of 0.5, 1 and 2 μM (Fig. 1D and E). According to these findings, PFG may inhibit MUC1 expression by decreasing MUC1 promoter activity in OC cells.

PFG suppresses the proliferation of OC cells. To understand the anticancer effect of PFG on OC cells, SKOV3 and A2780 cells were treated with PFG (0.5-40 μM) for 24, 48 and 72 h, and cell viability was detected by CCK-8 assay. According to the results, compared with in the control group, PFG suppressed the viability of SKOV3 and A2780 cells, and the inhibition was dose-dependent (Fig. 2A). The IC_{50} value at 24 h for SKOV3 cells was 10.79 μM, and the IC_{50} value at 24 h for A2780 cells was 3.845 μM. To rule out the potential bias in subsequent experiments caused by the cytotoxicity of high doses of PFG, 0.5, 1 and 2 μM concentrations were selected for subsequent experiments.

The EdU assay also indicated that PFG treatment inhibited the proliferation of both cell lines (Fig. 2B). Moreover, the colony formation assay revealed that PFG significantly inhibited the clonogenic ability of both cell lines (Fig. 2C).

To further assess the mechanism underlying the anti-proliferative effects of PFG, flow cytometry was performed to detect its effects on the apoptosis and cell cycle progression of the two cell lines. The results showed that in SKOV3 and A2780 cells, the apoptotic rate was significantly different in the PFG (2 μM) and docetaxel (80 nM) treatment groups compared with that in the control group (Fig. 3A), TUNEL detection indicated the same trend change in SKOV3 and A2780 cells (Fig. S1). However, the maximum apoptotic rate detected by the two experimental methods was <10%, which indicates that the effect of PFG on the apoptosis of SKOV3 and A2780 cells may have no biological significance. Cell cycle experiments demonstrated that PFG treatment could block the cell cycle in S phase, resulting in shortening of the G_0/G_1 phase and prolonging the S phase (Fig. 3B), with no significant change in the proportion of cells in G_2 phase. To explore the molecular mechanism underlying PFG-induced S-phase blockade, the expression levels of specific proteins associated with S-phase regulation were examined by western blotting. Notably, PFG treatment had a marked dose-dependent inhibitory effect on the protein expression levels of cyclin A, cyclin E and CDK2

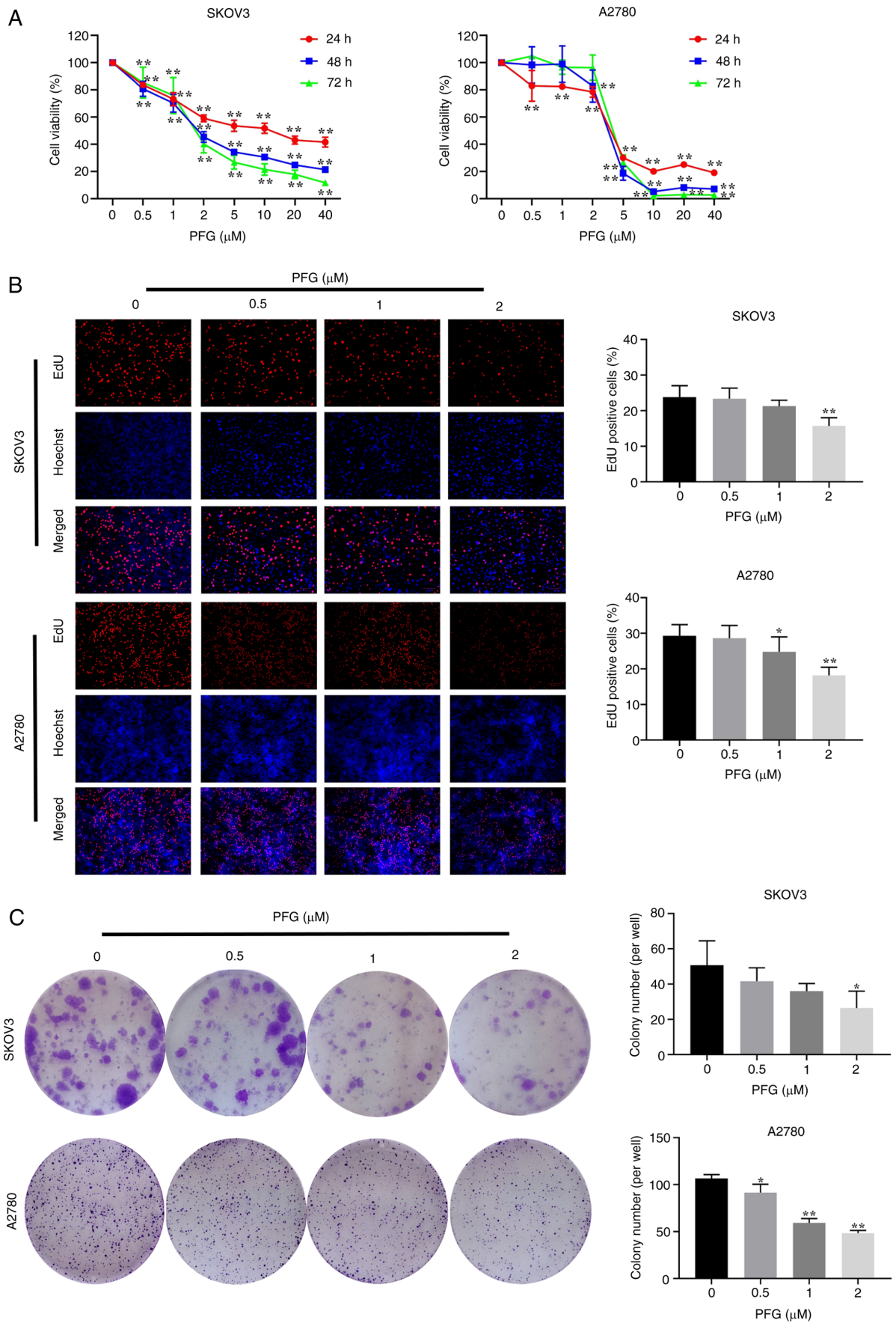

Figure 2. PFG suppresses the proliferation of ovarian cancer cells. (A) PFG was applied to SKOV3 and A2780 cells at concentrations of 0, 0.5, 1, 2, 5, 10, 20 and 40 μM. Cell viability was evaluated using the Cell Counting Kit-8 assay at 24, 48 and 72 h. (B) EdU assay measured the proliferation of SKOV3 and A2780 cells after 24 h of PFG treatment. Cells stained with red fluorescence indicated those that were in a proliferative state (magnification, x200). (C) Colony formation assay was performed to assess the clonogenic potential of PFG-treated SKOV3 and A2780 cells for 24 h. Data are presented as the mean ± SEM (n=3). One-way ANOVA was used to establish statistical significance. *P<0.05, **P<0.01 vs. control group. PFG, paeoniflorigenone.

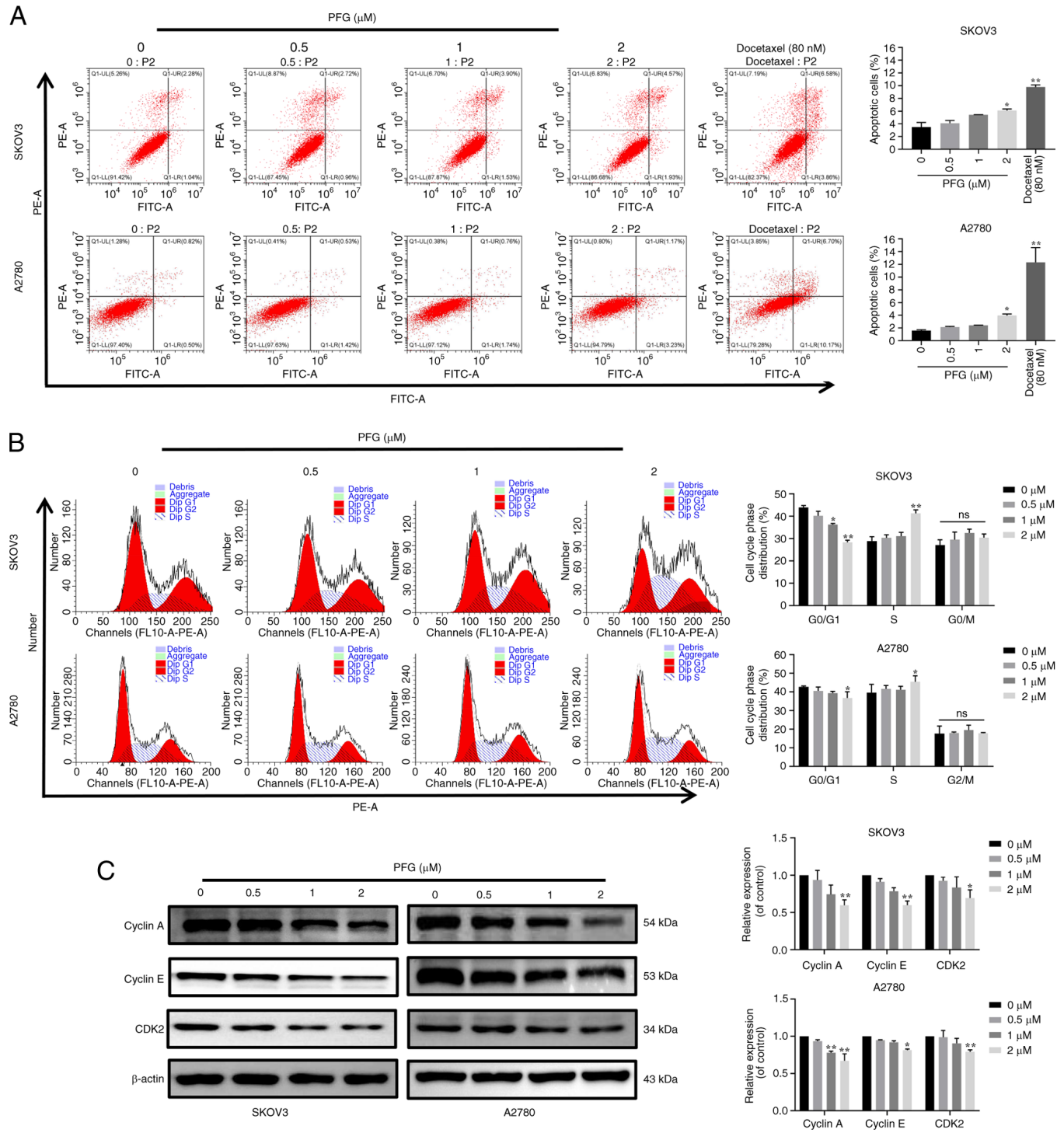

Figure 3. PFG induce S-phase arrest in OC cells. (A) Apoptotic rate (Q1-LR + Q1-UR) was measured after PFG treatment by flow cytometry. Docetaxel (80 nM) was used as a positive control drug. (B) Effects of PFG on the OC cell cycle were assessed using flow cytometry. (C) Cell cycle-related proteins cyclin A, cyclin E and CDK2 were subjected to western blot analysis to assess the effects of PFG treatment. Data are presented as the mean ± SEM (n=3). One-way ANOVA was used to establish statistical significance. *P<0.05, **P<0.01 vs. control group. ns, not significant; OC, ovarian cancer; PFG, paeoniflorigenone.

(Fig. 3C). These results suggested that PFG may induce S-phase cell cycle arrest in OC cell lines through controlling the levels of S-phase cell cycle regulatory proteins.

PFG suppresses cell migration, invasion and EMT in OC. OC frequently exhibits distant metastasis, and patients with metastatic OC exhibit a low survival rate when compared with primary OC (35). In order to determine if PFG has anti-metastatic effects, the migration of SKOV3 and A2780 cells was assessed using a wound-healing assay. Compared with in the control group, PFG significantly inhibited the migration of both cell lines in a dose-dependent manner (Fig. 4A). Furthermore, the effects of PFG on migration and invasion were assessed using the Transwell assay, and it was revealed that PFG markedly inhibited the migration and invasion of both cell lines in a dose-dependent manner (Fig. 4B).

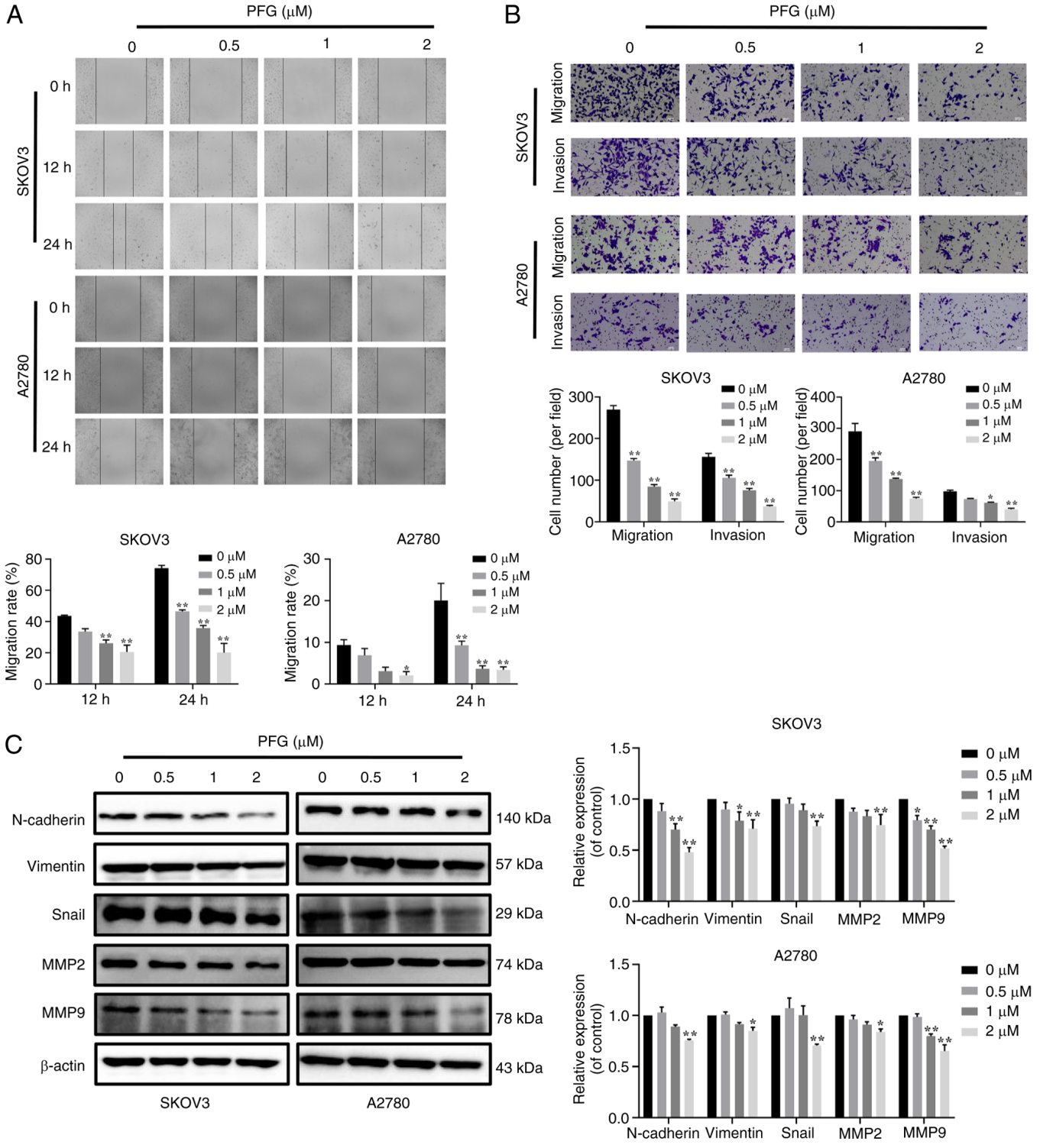

Figure 4. Functions of PFG on the migration, invasion and EMT of OC cells. (A) Cell migration was examined using the wound-healing assay and was observed under a light microscopy at 0, 12 and 24 h (magnification, x200); cell migration rate calculation using wound healing area. (B) Inhibitory effect of PFG on the ability of OC cells to invade and migrate, as identified using the Transwell assay (magnification, x200). (C) Inhibitory effect of PFG on EMT-related proteins (N-cadherin, Vimentin and Snail) and cell invasion-related proteins (MMP2 and MMP9) in OC cells was tested using a western blotting. Three independent repetitions of the experiment were performed. Data are presented as the mean ± SEM (n=3). One-way ANOVA was applied to establish statistical significance. *P<0.05, **P<0.01 vs. control group. EMT, epithelial-mesenchymal transition; OC, ovarian cancer; PFG, paeoniflorigenone.

Due to the importance of the EMT in the distant metastases of OC, identifying a new therapy that can target EMT is critical. To the best of our knowledge, the specific mechanism underlying the effects of PFG on the EMT of OC cells has not been reported. Therefore, after 24 h of PFG treatment, the expression levels of EMT-related proteins in the two OC cell lines were examined via western blot analysis. It was revealed that PFG could significantly inhibit the expression levels of MMP2 and MMP9, and downregulate the expression levels of mesenchymal markers, such as N-cadherin, Vimentin

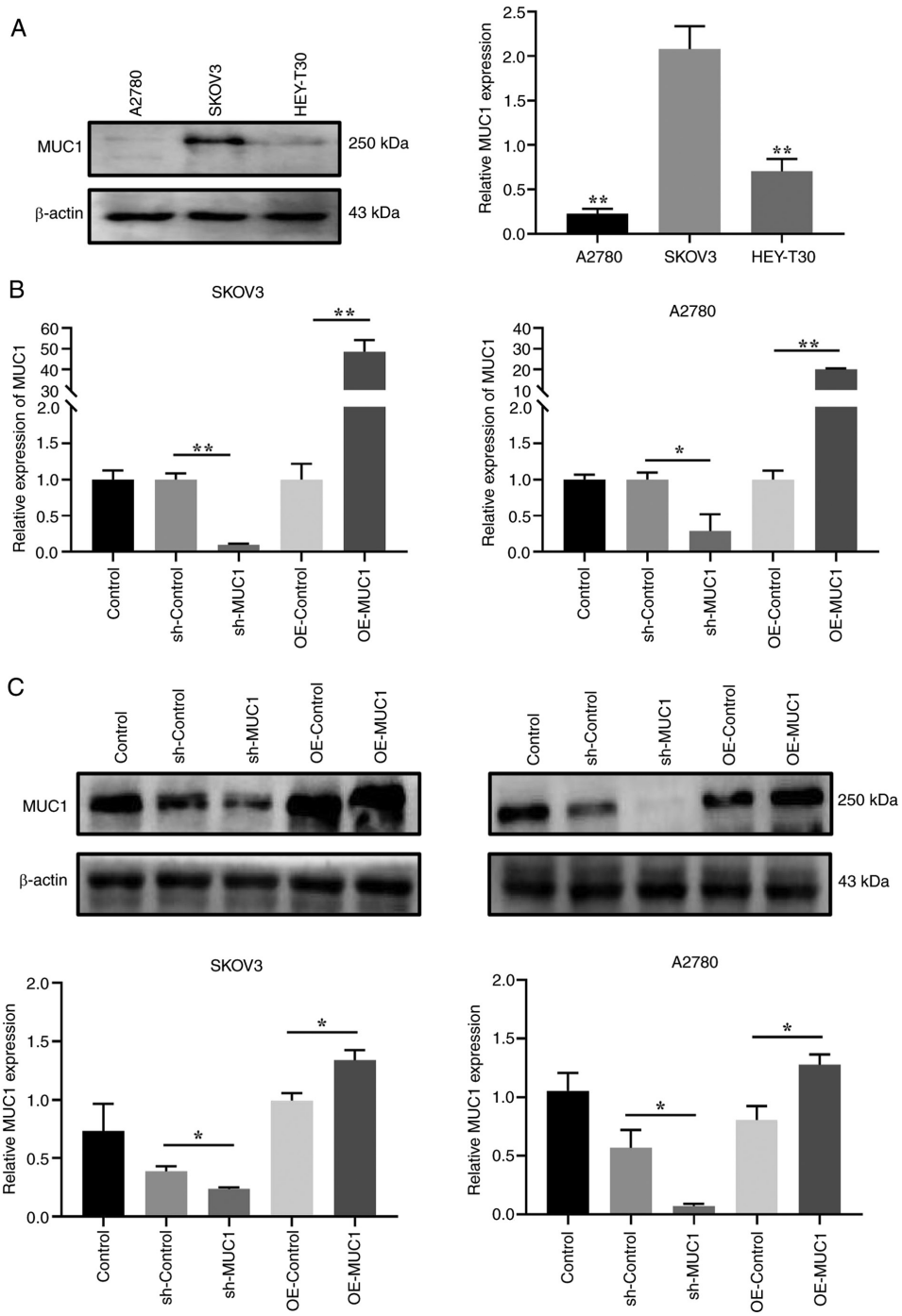

Figure 5. Construction of MUC1 knockdown and OE cell lines. (A) Comparison of the protein expression levels of MUC1 in three untreated human ovarian cancer cells. **P<0.01 vs. SKOV3. (B) Following lentiviral infection in SKOV3 and A2780 cells to produce cell lines with MUC1 knockdown and MUC1 OE, reverse transcription-quantitative polymerase chain reaction assays were performed to detect changes in MUC1 mRNA expression levels. (C) MUC1 protein expression levels post-infection with sh-MUC1 or MUC1 OE lentivirus plasmids in SKOV3 and A2780 cells were identified through western blotting. Data are presented as the mean ± SEM (n=3). One-way ANOVA was applied to establish statistical significance. *P<0.05, **P<0.01. MUC1, mucin 1; OE, overexpression; sh, short hairpin.

and Snail (Fig. 4C). These results indicated that PFG could block the activation of EMT in OC cells. Overall, it may be concluded that PFG suppresses OC cell migration and invasion via blocking EMT.

MUC1 promotes the proliferation of OC cells. To investigate the effects of MUC1 on OC cells, MUC1 protein expression levels were compared in three OC cell lines, and SKOV3 cells with the highest relative expression levels and A2780 cells with the lowest relative expression levels were selected for the construction of cells with stable MUC1 knockdown and overexpression for further mechanistic studies (Fig. 5A). Accordingly, RT-qPCR and western blot experiments verified the knockdown and overexpression of MUC1 (Fig. 5B and C). Compared with in the sh-Control cells, the results demonstrated that MUC1 knockdown had a significant effect on inhibiting the proliferation of OC cells (Fig. 6A and B), inducing cell cycle arrest at G_0/G_1 phase (Fig. 6C), and reducing

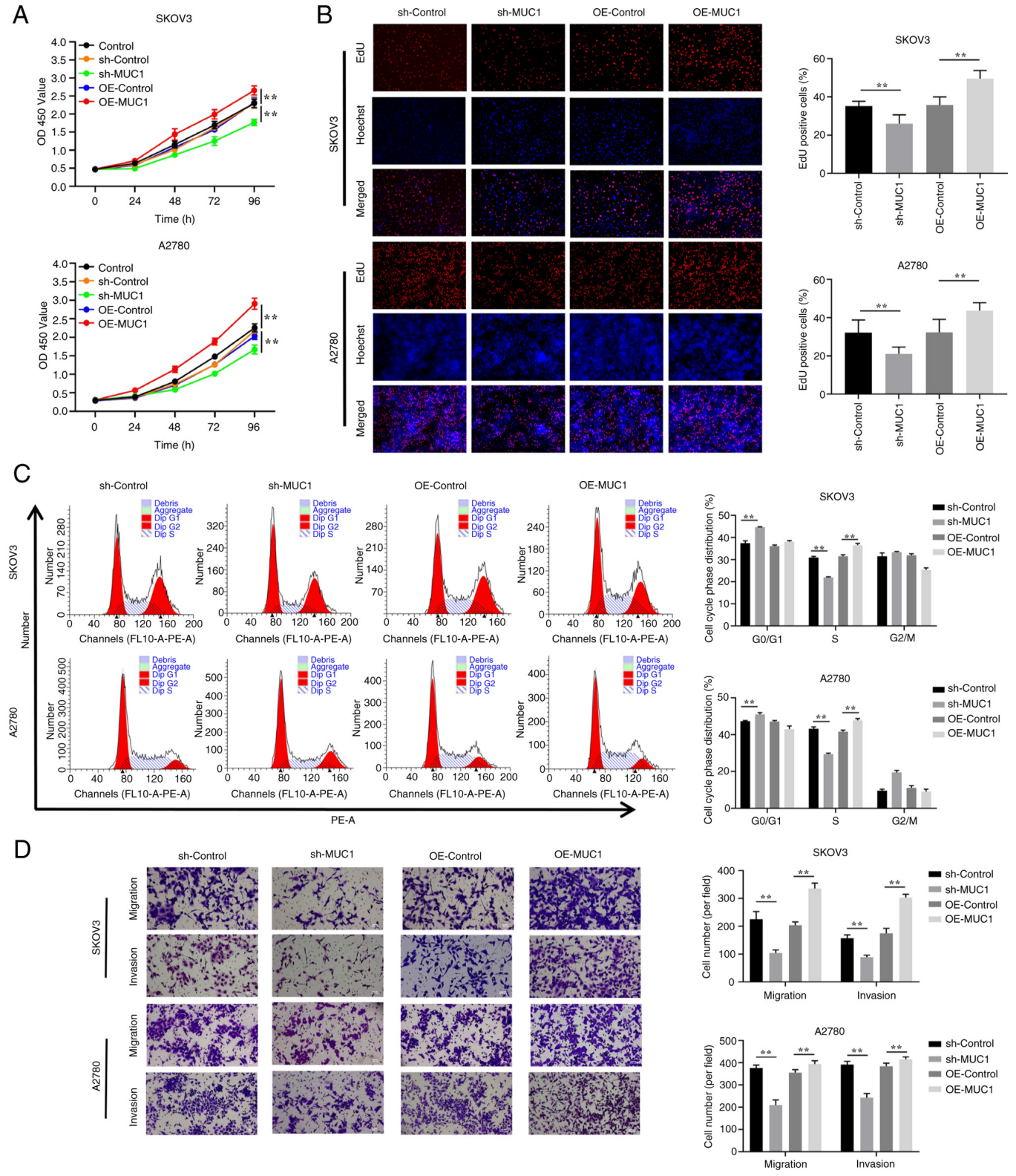

Figure 6. MUC1 promotes the proliferation of OC. (A) Proliferation curves of the two OC cell lines were affected by knockdown and OE of MUC1. The absorbance at 450 nm was measured at 0, 24, 48, 72 and 96 h using the Cell Counting Kit-8 assay. (B) Cell proliferation was discovered using the EdU assay and (C) cell cycle changes were assessed using flow cytometry. (D) Transwell assay was performed to determine cell migration and invasion (magnification, x200). Data are presented as the mean ± SEM (n=3). One-way ANOVA was applied to establish statistical significance. **P<0.01. MUC1, mucin 1; OC, ovarian cancer; OE, overexpression; sh, short hairpin.

cell migration and invasion (Fig. 6D). By contrast, compared with in the overexpression control (OE-control) cells, MUC1 overexpression promoted OC cell proliferation, accelerated cell cycle progression, and increased cell migration and invasion. These results implied that MUC1 is essential for OC cell proliferation and metastasis.

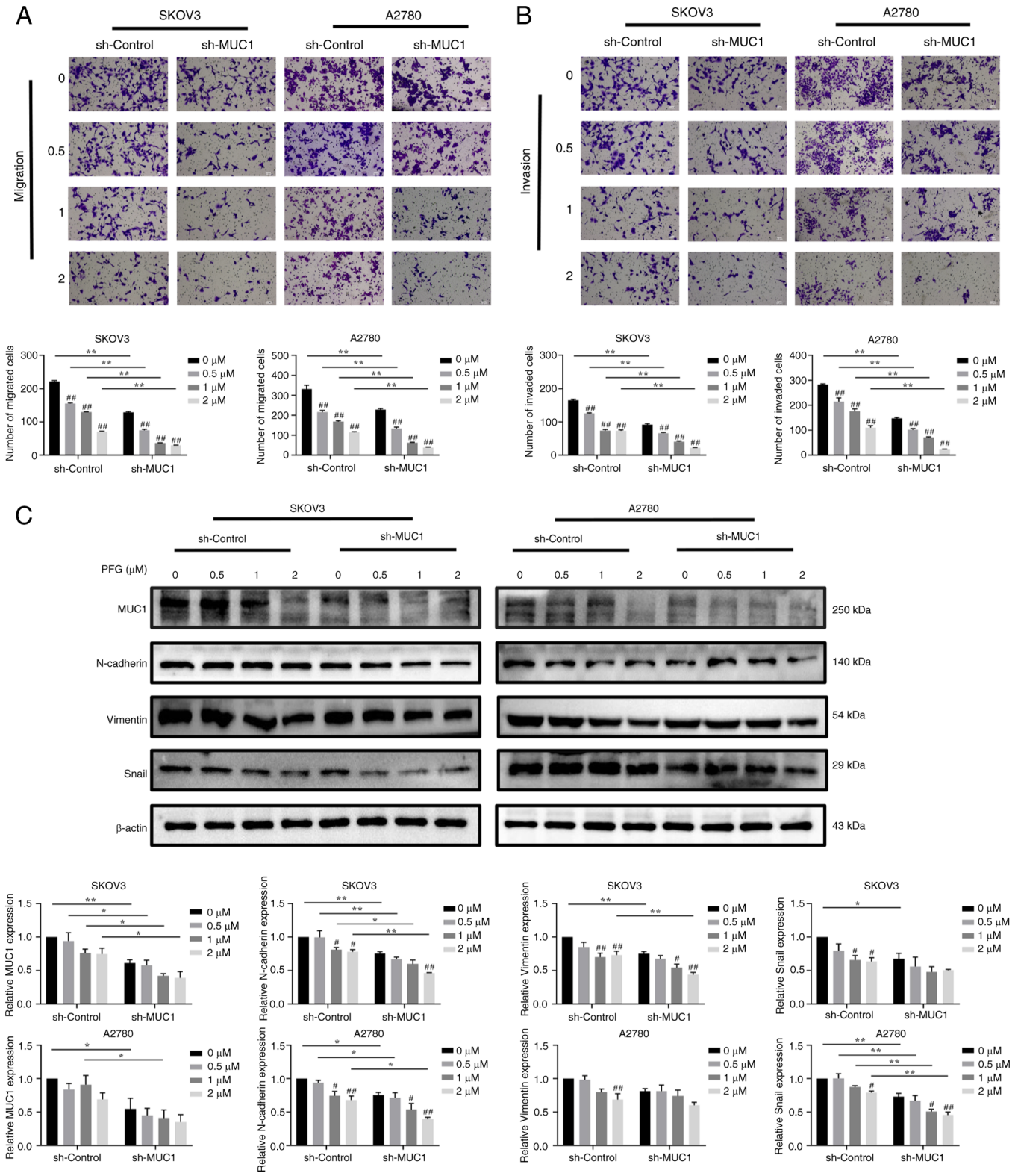

Figure 7. Knockdown of MUC1 in ovarian cancer cells enhances the inhibitory effects of PFG on tumor cell migration, invasion and EMT. SKOV3 and A2780 cells were incubated with PFG for 24 h at the given concentrations after being infected with a shRNA targeting MUC1. Transwell assay was employed to assess (A) migration and (B) invasion (magnification, x200). (C) MUC1 and EMT-related proteins were analyzed by western blotting, and the data were normalized to the sh-control or the OE-control group treated with 0 μM PFG. Data are presented as the mean ± SEM (n=3). Two-way ANOVA was applied to establish statistical significance. $^{\#}$P<0.05, $^{\#\#}$P<0.01 vs. control group (0 μM PFG); *P<0.05, **P<0.01. EMT, epithelial-mesenchymal transition; MUC1, mucin 1; PFG, paeoniflorigenone; sh, short hairpin.

PFG targets MUC1 to limit OC cell migration and invasion. To clarify whether PFG-induced antitumor effects were mediated by MUC1, the changes in migration and invasion were detected in cells with MUC1 knockdown and overexpression after treatment with various concentrations of PFG. The migration and invasion rate of sh-MUC1 cells was more

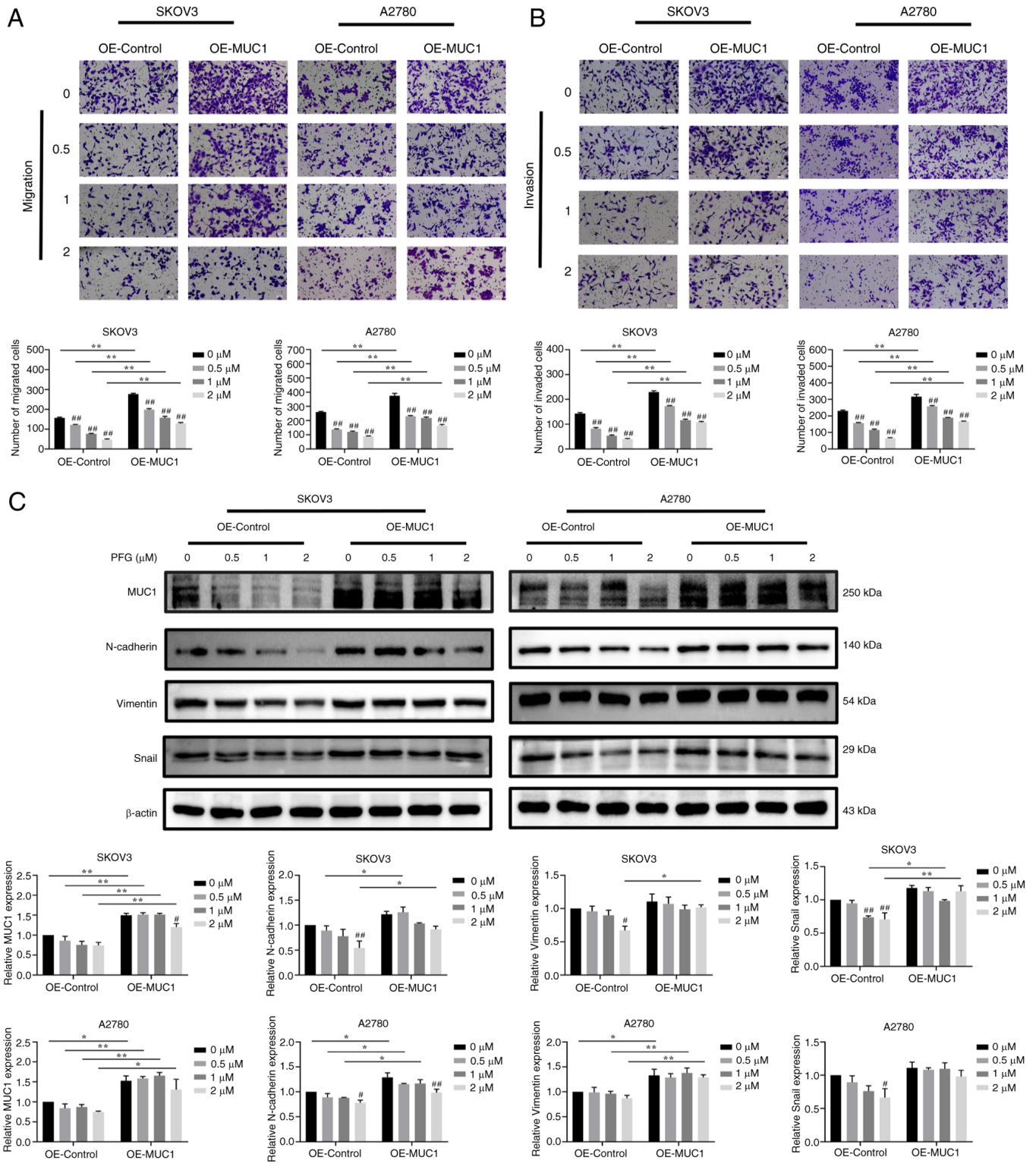

Figure 8. Overexpression of MUC1 in ovarian cancer cells antagonizes the antitumor effects of PFG. SKOV3 and A2780 cells were incubated with PFG for 24 h at the given concentrations after being infected with an overexpression vector targeting MUC1. Transwell assay was employed to assess (A) migration and (B) invasion (magnification, x200). (C) MUC1 and EMT-related proteins were analyzed by western blotting, and the data were normalized to the sh-control or the OE-control group treated with 0 μM PFG. Data are presented as the mean ± SEM (n=3). Two-way ANOVA was applied to establish statistical significance. $^{\#}$P<0.05, $^{\#\#}$P<0.01 vs. control group (0 μM PFG); *P<0.05, **P<0.01. EMT, epithelial-mesenchymal transition; MUC1, mucin 1; OE, overexpression; PFG, paeoniflorigenone.

affected by PFG than that of sh-control cells (Fig. 7A and B). Compared with the sh-control cells, in sh-MUC1 cells, the expression levels of MUC1 were significantly decreased and the inhibitory effect of PFG on EMT-related proteins (including N-cadherin, Vimentin and Snail) was enhanced (Fig. 7C).

By contrast, MUC1 overexpression restored and enhanced the migratory and invasive ability of SKOV3 and A2780 cells,

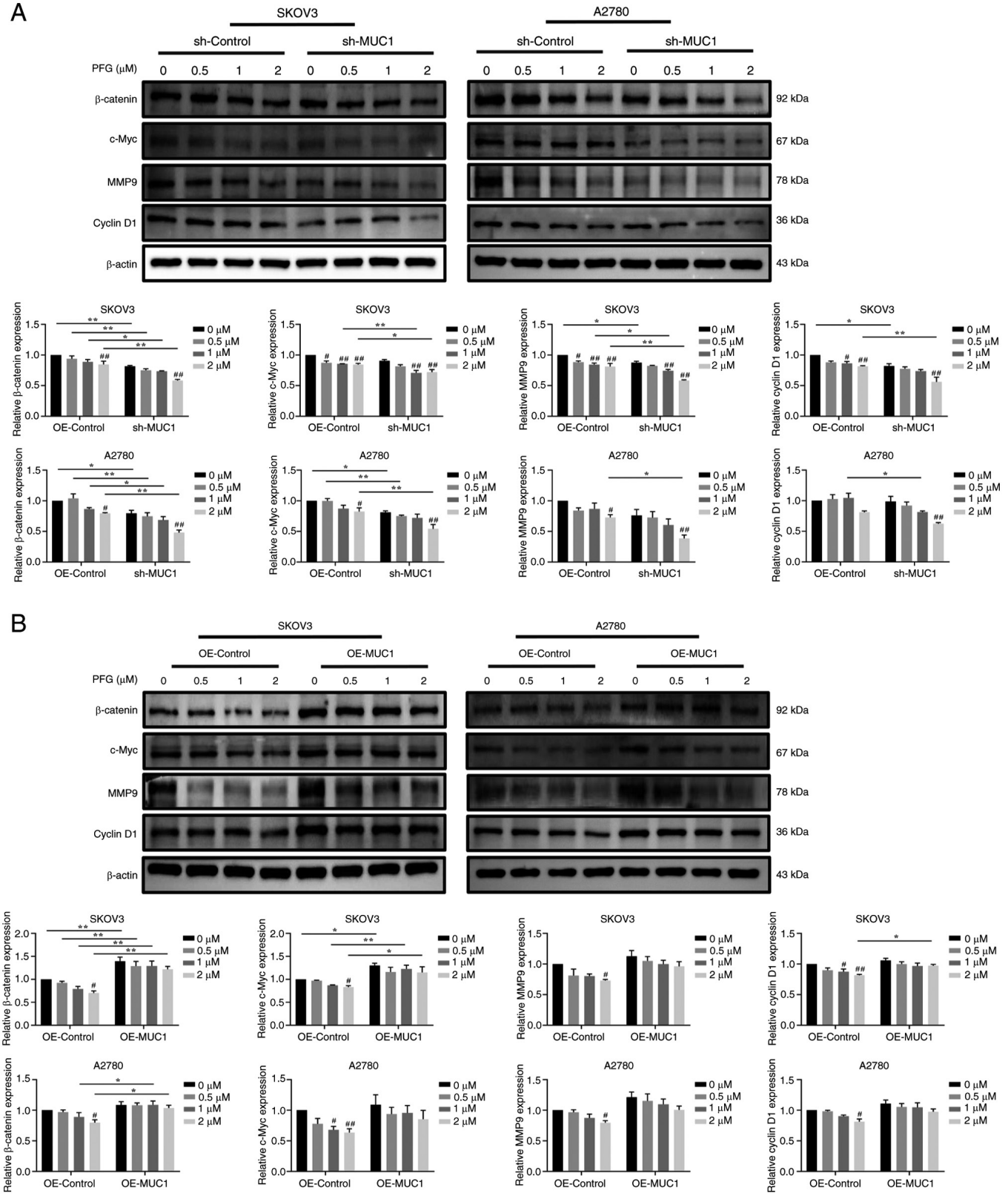

Figure 9. PFG blocks the Wnt/β-catenin signaling pathway via MUC1 suppression. Expression levels of key proteins in the Wnt signaling pathway and their downstream target proteins were measured in cells with MUC1 (A) knockdown and (B) OE by western blotting. PFG was applied to the cells for 24 h. Data are presented as the mean ± SEM (n=3) and the data were normalized to the sh-control or the OE-control group treated with 0 μM PFG. Two-way ANOVA was applied to establish statistical significance. $^{\#}$P<0.05, $^{\#\#}$P<0.01 vs. control group (0 μM PFG); *P<0.05, **P<0.01. MUC1, mucin 1; OE, overexpression; PFG, paeoniflorigenone; sh, short hairpin.

while also activating EMT. Compared with the OE-control cells, the inhibitory effect of different concentrations of PFG supplementation on cell migration and invasion was reduced in MUC1-overexpressing cells (Fig. 8A and B). Compared

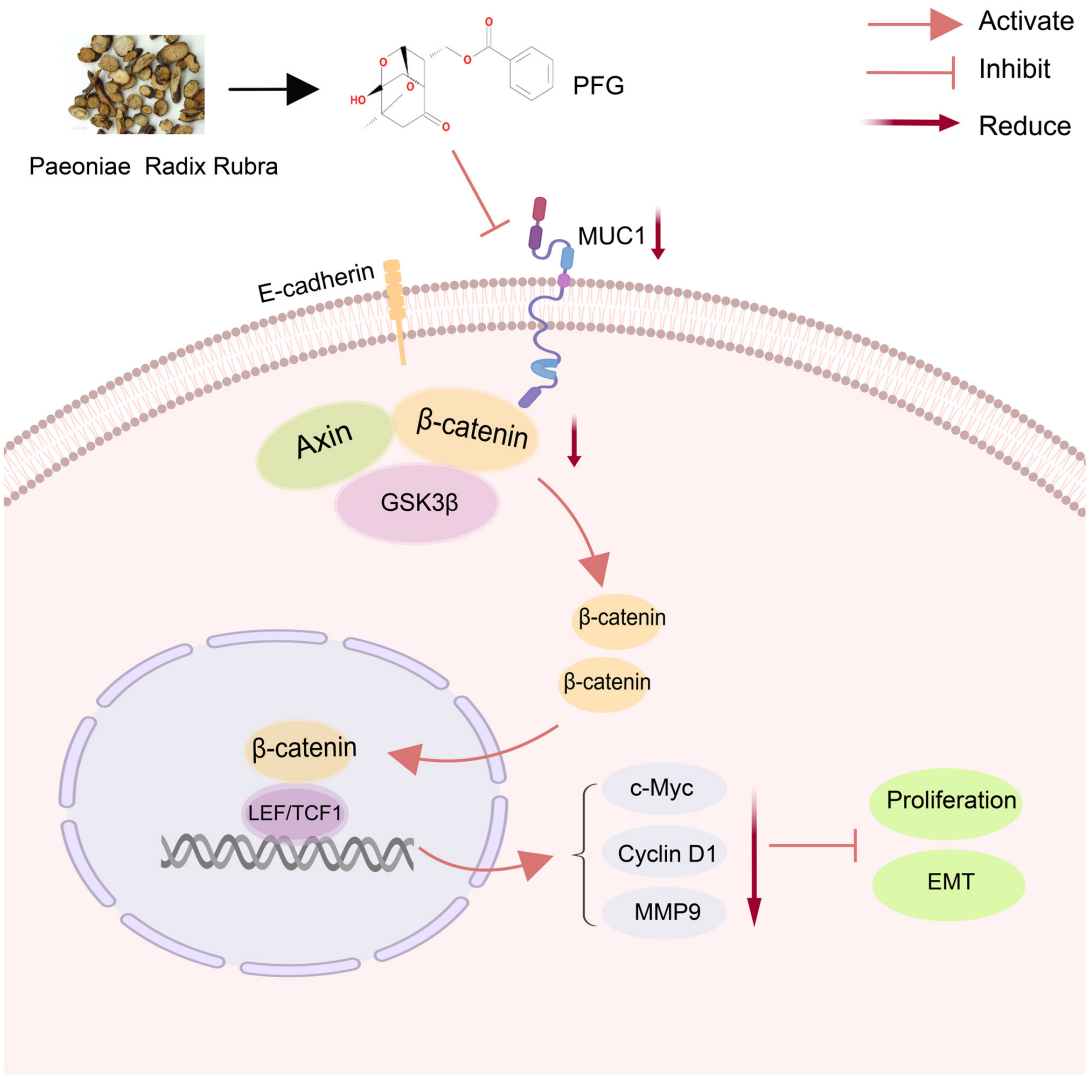

Figure 10. Graphic representation of the anticancer bioactivities of PFG in human ovarian cancer cells. EMT, epithelial-mesenchymal transition; MUC1, mucin 1; PFG, paeoniflorigenone.

with the OE-control cells, the expression levels of MUC1 were significantly increased in OE-MUC1 cells, and MUC1 overexpression partially reversed the PFG-induced decrease in N-cadherin, Vimentin and Snail protein expression levels. (Fig. 8C). These results indicated that MUC1 may be the dominant target protein through which PFG inhibits SKOV3 and A2780 cells migration, invasion and EMT.

PFG blocks the Wnt/β-catenin signaling pathway by inhibiting MUC1. The Wnt/β-catenin pathway is closely related to the migration and invasion of tumor cells (36). To evaluate the role of the Wnt/β-catenin pathway in the anti-OC effect of PFG, the Wnt/β-catenin pathway inhibitor XAV939 was used. Western blot analysis revealed that PFG and AXV939 exhibited similar inhibitory effects on SKOV3 and A2780 cells. The combination of PFG and XAV939 further suppressed the expression levels of β-catenin in SKOV3 cells, as well as the downstream target protein MMP9 in SKOV3 and A2780 cells (Fig. S2A). The results of the wound-healing assay showed that combining PFG and XAV939 markedly improved the inhibitory effect of PFG on OC cell migration (Fig. S2B). These results suggested that the Wnt/β-catenin pathway may have an important role in the inhibition of OC by PFG.

To elucidate whether PFG regulates the Wnt/β-catenin pathway and cancer motility via inhibiting the expression of MUC1, the protein expression levels of Wnt/β-catenin-related proteins and their downstream target proteins, which are linked to tumor cell metastasis and invasion were assessed. PFG (2 μM) treatment significantly reduced the protein expression levels of β-catenin, c-Myc, cyclin D1 and MMP9 in the sh-control cells and OE-control cells, when compared with the control cells (0 μM PFG), indicating that PFG inhibited Wnt/β-catenin pathway signaling in both OC cell lines. In addition, compared with sh-control cells, the silencing of MUC1 accelerated the decrease in β-catenin, c-Myc, MMP9 and cyclin D1 protein expression levels induced by PFG in SKOV3 and A2780 cells (Fig. 9A).

By contrast, compared with in the OE-control group, overexpression of MUC1 partially reversed the decrease in β-catenin protein expression levels in SKOV3 and A2780 cells induced by PFG, as well as c-Myc and cyclin D1 protein expression levels in SKOV3 cells (Fig. 9B). In summary, it may be

suggested that PFG can prevent the EMT process by blocking the Wnt/β-catenin signaling pathway through inhibiting MUC1 in OC cells (Fig. 10).

Discussion

The present study indicated that PFG can inhibit the proliferation of OC cells, induce cell cycle arrest in the S phase, and suppress cell migration and invasion. Moreover, PFG inhibited the promoter activity of MUC1, lowered its protein expression, and suppressed the production of crucial proteins in the Wnt/β-catenin signaling pathway.

PFG has been shown in several studies to reduce the proliferative capacity of tumor cells, and is cytotoxic and selectively induces apoptosis in cancer cell lines (20,21); notably, the present study confirmed these effects in two OC cell lines. The latest research shows that PFG exerts anticancer effects by inducing apoptotic cell death and blocking metastatic processes via the inactivation of PI3K/AKT/mTOR/p70S6K signaling (37). In the present study, although PFG significantly affected the apoptotic rate of OC cells, the maximum apoptotic rate was <10% in both flow cytometry and TUNEL experiments, which is not biologically significant, suggesting that when the survival rate of SKOV3 and A2780 cells is >80%, induction of apoptosis is not the primary mechanism by which PFG inhibits OC cells. Subsequently, it was revealed that PFG significantly inhibited the expression levels of the cell cycle-related proteins cyclin A, cyclin E and CDK2, leading to cell cycle arrest in S phase. This could be one of the key reasons why PFG inhibits the proliferation of OC cells. Furthermore, MUC1 knockdown caused cell cycle arrest in the G_0/G_1 phase, which differed from the direct action of PFG on OC cells. PFG has previously been shown to lower the expression of cyclin D1, CDK4 and CDK6 in tumor cells, which may affect progression of the G_1 phase (37); however, another study demonstrated that PFG can promote S-phase arrest in HeLa cells (21). These findings indicated that the regulatory effects of PFG on cells is multifaceted. Although the present study demonstrated that PFG can directly bind to MUC1, it is also plausible that PFG interacts with other molecules at the same time, influencing cell cycle-related protein expression. The results of the present study showed that PFG only significantly affected S phase in SKOV3 and A2780 cells.

Cancer cell expansion, motility, invasion and EMT are associated with MUC1. In the present study, knockdown and overexpression of MUC1 in OC cells confirmed its crucial function in OC progression, which is consistent with previous research (38-40). Research on MUC1 has increased as a result of its promise as an OC therapeutic target. For example, it has been suggested that patients with EOC may have a higher chance of overall survival if IgG antibodies to MUC1 are induced (41). Furthermore, the anti-MUC1 monoclonal antibody C595 alone, and in combination with docetaxel, greatly improves the efficiency of OC cell death and induces apoptosis (42,43). Moreover, the new vaccine BN-CV301, which encodes the tumor-associated antigens MUC1 and CEA, induces T-cell responses to these antigens, resulting in high levels of immunogenicity that may have therapeutic benefits either alone or in combination with anti-PD-1/L1 drugs (44-46). These results offer an experimental foundation for ongoing preclinical assessment of MUC1 targeting. GO-203, a cell-penetrating peptide-based MUC1-cytoplasmic tail (CT) inhibitor, is still in phase I clinical trials for the treatment of breast cancer (25). However, there are currently few targeted drugs that target MUC1, and PFG, a monomer compound of traditional Chinese medicine, is expected to be a good candidate inhibitor of MUC1. The present study discovered that the TCM compound PFG directly inhibited MUC1 expression, and that knocking down MUC1 via external intervention further enhanced its efficacy. By contrast, MUC1 overexpression antagonized the antitumor activity of PFG. As a result, it may be hypothesized that MUC1 is a critical target for PFG to exert its anticancer effects. More investigation is warranted to determine which region of PFG primarily binds to MUC1 and affects its function.

A complex between β-catenin and T cell-specific transcription factor that drives transcriptional activity is formed as a result of the Wnt/β-catenin pathway. Notably, the onset, development, progression and worsening of numerous malignancies are linked to elevated transcriptional activity of this pathway (47-49). Recent research has demonstrated that cancer cell migration can be inhibited and the Wnt/β-catenin signaling pathway can be blocked by MUC1 silencing (50). Furthermore, interfering with MUC1 via small interfering RNA can decrease the interaction between MUC1-CT and β-catenin, inhibiting β-catenin nuclear translocation and target gene expression during carcinogenesis (51,52).

During the present study, it was revealed that the Wnt/β-catenin pathway is critical in the inhibition of OC by PFG. Furthermore, PFG and the pathway inhibitor XAV939 had a similar inhibitory effect on OC cell migration, and their combination considerably increased the inhibitory effects of PFG. Moreover, it was revealed that the expression levels of key Wnt/β-catenin pathway proteins, including β-catenin, and critical downstream genes, such as c-Myc, MMP9 and cyclin D1, were significantly altered in two OC cell lines with MUC1 knockdown and overexpression. Additionally, it was observed that PFG treatment inhibited this pathway more effectively in cells with MUC1 knockdown and less effectively in MUC1-overexpressing cells. Taken together, it may be hypothesized that PFG can prevent OC cell migration and invasion by decreasing MUC1 expression and blocking the Wnt/β-catenin signaling pathway. PFG could be used as an effective inhibitor targeting MUC1, providing a new experimental basis for the treatment of OC with TCM.

The present study investigated the antitumor activity of PFG against OC. The binding relationship between PFG and its target MUC1 was identified, and further experiments were performed to assess how MUC1 expression affects PFG efficacy. The detailed mechanistic investigation revealed that PFG may exert anti-migratory, -invasive and -EMT effects on OC by preventing MUC1 from being expressed and thus suppressing the Wnt/β-catenin signaling pathway. These results indicated that a possible therapeutic option for OC is MUC1, and PFG could be used to treat OC as a MUC1 inhibitor. However, there are several limitations to the present study that require further exploration: i) Only the inhibitory effect of PFG on EOC cells was investigated, suggesting that other types of OC may involve different mechanisms; ii) further extensive investigations are essential to explore the inhibitory mechanism of PFG

on MUC1; and iii) additional *in vivo* experiments are needed to support the findings of this study. iv) In addition, the specific mechanism of PFG-induced S-phase arrest of OC cells needs to be further explored.

Acknowledgements

Not applicable.

Funding

The present study was supported by the National Natural Science Foundation of China (grant nos. 82074391 and 82204875), the Zhejiang Provincial Natural Science Foundation of China (grant nos. LY21H270004 and LQ23H270012), the Youth Project of Guangdong Basic and Applied Basic Regional Joint Fund (grant no. 2020A1515110281), and the Graduate Research Foundation of Zhejiang Chinese Medical University (grant no. 2021YKJ19).

Availability of data and materials

The datasets used and/or analyzed during the current study are available from the corresponding author on reasonable request.

Authors' contributions

FT and YX designed the study, revised the manuscript and finalized the article. QL performed experiments and wrote the manuscript. QL and LJ collected and analyzed the data. YZ and FS performed the statistical analysis. XT, WL, JL and XJ contributed to data analysis and interpretation. QL and LJ confirm the authenticity of all the raw data. All authors read and approved the final manuscript.

Ethics approval and consent to participate

Not applicable.

Patient consent for publication

Not applicable.

Competing interest

The authors declare that they have no competing interests.

References

1. Coburn SB, Bray F, Sherman ME and Trabert B: International patterns and trends in ovarian cancer incidence, overall and by histologic subtype. Int J Cancer 140: 2451-2460, 2017.
2. Torre LA, Bray F, Siegel RL, Ferlay J, Lortet-Tieulent J and Jemal A: Global cancer statistics, 2012. CA Cancer J Clin 65: 87-108, 2015.
3. Siegel RL, Miller KD, Wagle NS and Jemal A: Cancer statistics, 2023. CA Cancer J Clin 73: 17-48, 2023.
4. Colombo N, Peiretti M, Parma G, Lapresa M, Mancari R, Carinelli S, Sessa C and Castiglione M; ESMO Guidelines Working Group: Newly diagnosed and relapsed epithelial ovarian carcinoma: ESMO Clinical Practice Guidelines for diagnosis, treatment and follow-up. Ann Oncol 21 (Suppl 5): v23-v30, 2010.
5. Coleman RL, Monk BJ, Sood AK and Herzog TJ: Latest research and treatment of advanced-stage epithelial ovarian cancer. Nat Rev Clin Oncol 10: 211-224, 2013.
6. Ediriweera MK, Tennekoon KH and Samarakoon SR: Role of the PI3K/AKT/mTOR signaling pathway in ovarian cancer: Biological and therapeutic significance. Semin Cancer Biol 59: 147-160, 2019.
7. Christie EL and Bowtell DDL: Acquired chemotherapy resistance in ovarian cancer. Ann Oncol 28 (suppl_8): viii13-viii15, 2017.
8. Wang Y, Zhang Q, Chen Y, Liang CL, Liu H, Qiu F and Dai Z: Antitumor effects of immunity-enhancing traditional Chinese medicine. Biomed Pharmacother 121: 109570, 2020.
9. Sun Z, Su YH and Yue XQ: Professor ling Changquan's experience in treating primary liver cancer: An analysis of herbal medication. Zhong Xi Yi Jie He Xue Bao 6: 1221-1225, 2008 (In Chinese).
10. Tian AP, Yin YK, Yu L, Yang BY, Li N, Li JY, Bian ZM, Hu SY, Weng CX and Feng L: Low-Frequency sonophoresis of chinese medicine formula improves efficacy of malignant pleural effusion treatment. Chin J Integr Med 26: 263-269, 2020.
11. Gao J, Yang J, Lu Z, Dong X and Xu Y: The Multiple pharmacologic functions and mechanisms of action of guizhi fuling formulation. Evid Based Complement Alternat Med 2022: 6813421, 2022.
12. Yang J, Ren Y, Lou ZG, Wan X, Weng GB and Cen D: Paeoniflorin inhibits the growth of bladder carcinoma via deactivation of STAT3. Acta Pharm 68: 211-222, 2018.
13. Liu H, Zang L, Zhao J, Wang Z and Li L: Paeoniflorin inhibits cell viability and invasion of liver cancer cells via inhibition of Skp2. Oncol Lett 19: 3165-3172, 2020.
14. Zheng YB, Xiao GC, Tong SL, Ding Y, Wang QS, Li SB and Hao ZN: Paeoniflorin inhibits human gastric carcinoma cell proliferation through up-regulation of microRNA-124 and suppression of PI3K/Akt and STAT3 signaling. World J Gastroenterol 21: 7197-7207, 2015.
15. Wang Y, Wang Q, Li X, Luo G, Shen M, Shi J, Wang X and Tang L: Paeoniflorin Sensitizes breast cancer cells to tamoxifen by Downregulating microRNA-15b via the FOXO1/CCND1/β-Catenin axis. Drug Des Devel Ther 15: 245-257, 2021.
16. Gao J, Song L, Xia H, Peng L and Wen Z: 6'-O-galloylpaeoniflorin regulates proliferation and metastasis of non-small cell lung cancer through AMPK/miR-299-5p/ATF2 axis. Respir Res 21: 39, 2020.
17. Wang XZ, Xia L, Zhang XY, Chen Q, Li X, Mou Y, Wang T and Zhang YN: The multifaceted mechanisms of Paeoniflorin in the treatment of tumors: State-of-the-Art. Biomed Pharmacother 149: 112800, 2022.
18. Kimura M, Kimura I, Nojima H, Takahashi K, Hayashi T, Shimizu M and Morita N: Blocking effects of a new component, paeoniflorigenone, in paeony root on neuromuscular junctions of frogs and mice. Jpn J Pharmacol 35: 61-66, 1984.
19. Koo YK, Kim JM, Koo JY, Kang SS, Bae K, Kim YS, Chung JH and Yun-Choi HS: Platelet anti-aggregatory and blood anti-coagulant effects of compounds isolated from *Paeonia lactiflora* and Paeonia suffruticosa. Pharmazie 65: 624-628, 2010.
20. Huang Y, Ohno O, Suenaga K and Miyamoto K: Apoptosis-inducing activity and antiproliferative effect of Paeoniflorigenone from moutan cortex. Biosci Biotechnol Biochem 81: 1106-1113, 2017.
21. Huang Y, Ohno O and Miyamoto K: PFG acted as an inducer of premature senescence in TIG-1 normal diploid fibroblast and an inhibitor of mitosis in the HeLa cells. Biosci Biotechnol Biochem 83: 986-995, 2019.
22. Hu XF, Yang E, Li J and Xing PX: MUC1 cytoplasmic tail: A potential therapeutic target for ovarian carcinoma. Expert Rev Anticancer Ther 6: 1261-1271, 2006.
23. Van Elssen CH, Frings PW, Bot FJ, Van de Vijver KK, Huls MB, Meek B, Hupperets P, Germeraad WT and Bos GM: Expression of aberrantly glycosylated Mucin-1 in ovarian cancer. Histopathology 57: 597-606, 2010.
24. Gendler SJ: MUC1, the renaissance molecule. J Mammary Gland Biol Neoplasia 6: 339-353, 2001.
25. Nath S and Mukherjee P: MUC1: A multifaceted oncoprotein with a key role in cancer progression. Trends Mol Med 20: 332-342, 2014.
26. Chen W, Zhang Z, Zhang S, Zhu P, Ko JK and Yung KK: MUC1: Structure, function, and clinic application in epithelial cancers. Int J Mol Sci 22: 6567, 2021.

27. Mommers EC, Leonhart AM, von Mensdorff-Pouilly S, Schol DJ, Hilgers J, Meijer CJ, Baak JP and van Diest PJ: Aberrant expression of MUC1 mucin in ductal hyperplasia and ductal carcinoma In situ of the breast. Int J Cancer 84: 466-469, 1999.
28. Gaemers IC, Vos HL, Volders HH, van der Valk SW and Hilkens J: A stat-responsive element in the promoter of the episialin/MUC1 gene is involved in its overexpression in carcinoma cells. J Biol Chem 276: 6191-6199, 2001.
29. Wesseling J, van der Valk SW, Vos HL, Sonnenberg A and Hilkens J: Episialin (MUC1) overexpression inhibits integrin-mediated cell adhesion to extracellular matrix components. J Cell Biol 129: 255-265, 1995.
30. Feng H, Ghazizadeh M, Konishi H and Araki T: Expression of MUC1 and MUC2 mucin gene products in human ovarian carcinomas. Jpn J Clin Oncol 32: 525-529, 2002.
31. Mohr AM, Bailey JM, Lewallen ME, Liu X, Radhakrishnan P, Yu F, Tapprich W and Hollingsworth MA: MUC1 regulates expression of multiple microRNAs involved in pancreatic tumor progression, including the miR-200c/141 cluster. PLoS One 8: e73306, 2013.
32. Rajabi H, Alam M, Takahashi H, Kharbanda A, Guha M, Ahmad R and Kufe D: MUC1-C oncoprotein activates the ZEB1/miR-200c regulatory loop and epithelial-mesenchymal transition. Oncogene 33: 1680-1689, 2014.
33. Seeliger D and de Groot BL: Ligand docking and binding site analysis with PyMOL and Autodock/Vina. J Comput Aided Mol Des 24: 417-422, 2010.
34. Livak KJ and Schmittgen TD: Analysis of relative gene expression data using real-time quantitative PCR and the 2(-Delta Delta C(T)) method. Methods 25: 402-408, 2001.
35. Gardner AB, Charo LM, Mann AK, Kapp DS, Eskander RN and Chan JK: Ovarian, uterine, and cervical cancer patients with distant metastases at diagnosis: Most common locations and outcomes. Clin Exp Metastasis 37: 107-113, 2020.
36. Zhao H, Ming T, Tang S, Ren S, Yang H, Liu M, Tao Q and Xu H: Wnt signaling in colorectal cancer: Pathogenic role and therapeutic target. Mol Cancer 21: 144, 2022.
37. Park KR, Lee H, Kim SH and Yun HM: Paeoniflorigenone regulates apoptosis, autophagy, and necroptosis to induce anti-cancer bioactivities in human head and neck squamous cell carcinomas. J Ethnopharmacol 288: 115000, 2022.
38. Wang L, Ma J, Liu F, Yu Q, Chu G, Perkins AC and Li Y: Expression of MUC1 in primary and metastatic human epithelial ovarian cancer and its therapeutic significance. Gynecol Oncol 105: 695-702, 2007.
39. Deng J, Wang L, Chen H, Li L, Ma Y, Ni J and Li Y: The role of tumour-associated MUC1 in epithelial ovarian cancer metastasis and progression. Cancer Metastasis Rev 32: 535-551, 2013.
40. Ma Q, Song J, Wang S and He N: MUC1 regulates AKT signaling pathway by upregulating EGFR expression in ovarian cancer cells. Pathol Res Pract 224: 153509, 2021.
41. Oei AL, Moreno M, Verheijen RH, Sweep FC, Thomas CM, Massuger LF and von Mensdorff-Pouilly S: Induction of IgG antibodies to MUC1 and survival in patients with epithelial ovarian cancer. Int J Cancer 123: 1848-1853, 2008.
42. Wang L, Chen H, Liu F, Madigan MC, Power CA, Hao J, Patterson KI, Pourgholami MH, O'Brien PM, Perkins AC and Li Y: Monoclonal antibody targeting MUC1 and increasing sensitivity to docetaxel as a novel strategy in treating human epithelial ovarian cancer. Cancer Lett 300: 122-133, 2011.
43. Wang L, Chen H, Pourgholami MH, Beretov J, Hao J, Chao H, Perkins AC, Kearsley JH and Li Y: Anti-MUC1 monoclonal antibody (C595) and docetaxel markedly reduce tumor burden and ascites, and prolong survival in an in vivo ovarian cancer model. PLoS One 6: e24405, 2011.
44. Mohebtash M, Tsang KY, Madan RA, Huen NY, Poole DJ, Jochems C, Jones J, Ferrara T, Heery CR, Arlen PM, *et al*: A pilot study of MUC-1/CEA/TRICOM poxviral-based vaccine in patients with metastatic breast and ovarian cancer. Clin Cancer Res 17: 7164-7173, 2011.
45. Morse MA, Niedzwiecki D, Marshall JL, Garrett C, Chang DZ, Aklilu M, Crocenzi TS, Cole DJ, Dessureault S, Hobeika AC, *et al*: A randomized phase II study of immunization with dendritic cells modified with poxvectors encoding CEA and MUC1 compared with the same poxvectors plus GM-CSF for resected metastatic colorectal cancer. Ann Surg 258: 879-886, 2013.
46. Gatti-Mays ME, Strauss J, Donahue RN, Palena C, Del Rivero J, Redman JM, Madan RA, Marté JL, Cordes LM, Lamping E, *et al*: A phase I Dose-escalation trial of BN-CV301, a recombinant poxviral vaccine targeting MUC1 and CEA with costimulatory molecules. Clin Cancer Res 25: 4933-4944, 2019.
47. Tsuchiya K, Kiyoshi M, Hashii N, Fujita M, Kurohara T, Ishii-Watabe A, Fukuhara K, Misawa T and Demizu Y: Development of a penetratin-conjugated stapled peptide that inhibits Wnt/β-catenin signaling. Bioorg Med Chem 73: 117021, 2022.
48. Zhang Y and Wang X: Targeting the Wnt/β-catenin signaling pathway in cancer. J Hematol Oncol 13: 165, 2020.
49. Liu J, Xiao Q, Xiao J, Niu C, Li Y, Zhang X, Zhou Z, Shu G and Yin G: Wnt/β-catenin signalling: Function, biological mechanisms, and therapeutic opportunities. Signal Transduct Target Ther 7: 3, 2022.
50. Song F, Chen FY, Wu SY, Hu B, Liang XL, Yang HQ, Cheng JW, Wang PX, Guo W, Zhou J, *et al*: Mucin 1 promotes tumor progression through activating WNT/β-catenin signaling pathway in intrahepatic cholangiocarcinoma. J Cancer 12: 6937-6947, 2021.
51. Liu X, Caffrey TC, Steele MM, Mohr A, Singh PK, Radhakrishnan P, Kelly DL, Wen Y and Hollingsworth MA: MUC1 regulates cyclin D1 gene expression through p120 catenin and β-catenin. Oncogenesis 3: e107, 2014.
52. Wang Z, Sun J, Hu X and Huang S: Interference of mucin 1 inhibits progression of colon carcinoma by repression of Wnt/β-catenin signaling. DNA Cell Biol 33: 162-170, 2014.